



## RESEARCH ARTICLE

### Immunoinformatics-Driven Engineering of a Chimeric E0/E2 Epitope Vaccine Targeting Bovine Viral Diarrhea Virus

Shaobo Liang<sup>1</sup>, Min Wei<sup>1</sup>, Weijie Zhou<sup>1</sup>, and Feng Pang<sup>1\*</sup>

<sup>1</sup>Department of Veterinary Medicine, College of Animal Science, Guizhou University, Guiyang 550025, China

\*Corresponding author: fpang@gzu.edu.cn

#### ARTICLE HISTORY (25-311)

Received: April 13, 2025

Revised: June 14, 2025

Accepted: June 16, 2025

Published online: July 14, 2025

#### Key words:

BVDV

Immune simulation

Immuno-informatics

Molecular docking

Multi-epitope vaccine

#### ABSTRACT

Bovine viral diarrhea virus (BVDV) poses substantial economic burdens to global cattle industries. To address this, we designed an innovative multi-epitope vaccine targeting BVDV via immuno-informatics. Seven cytotoxic T lymphocyte (CTL), five helper T lymphocyte (HTL), and seven B-cell epitopes from E0/E2 glycoproteins were strategically connected using AAY, GPGPG, and KK linkers. To boost immunogenicity, a  $\beta$ -defensin adjuvant was incorporated at the N-terminal of the vaccine using a short peptide linker EAAAK. Computational analysis confirmed favorable physiochemical properties, antigenicity, solubility, and safety (non-allergenic, non-toxic). Structural optimization yielded a stable vaccine's 3D model with improved Z-score (-2.67). Molecular docking revealed strong interactions between the vaccine and bovine TLR2 and TLR4. Molecular dynamics analysis confirmed the stability of the docked vaccine-TLR complexes. Immune simulation predicted robust humoral responses (elevated IgG/IgM) and cellular immunity (increased IFN- $\gamma$ /IL-2). The codon-optimized sequence showed significant potential for high-level expression in *E. coli*. The newly designed chimeric E0/E2 epitope vaccine shows promise for triggering dual immune responses, offering a viable strategy for BVDV control.

**To Cite This Article:** Liang S, Wei M, Zhou W and Pang F, 2025. Immunoinformatics-driven engineering of a chimeric E0/E2 epitope vaccine targeting bovine viral diarrhea virus. Pak Vet J, 45(3): 1199-1207. <http://dx.doi.org/10.29261/pakvetj/2025.201>

#### INTRODUCTION

Bovine viral diarrhea virus (BVDV), a member of the *Pestivirus* genus within the *Flaviviridae* family, is a major cattle pathogen causing global economic losses (Newcomer, 2021). Its clinical manifestations range from acute diarrhea, respiratory distress, and reproductive issues (such as abortions and infertility) to immunosuppression, though subclinical infections are common (Lanyon *et al.*, 2014). BVDV comprises two biotypes classified by cytopathic effects in cell cultures. Non-cytopathic (ncp) strains dominate and evade host immunity to establish persistent infections, while cytopathic (cp) variants induce cell death and correlate with acute clinical manifestations (Miroslaw *et al.*, 2022). Early gestational exposure to ncp BVDV strains may induce persistent infection (PI), with PI calves becoming lifelong viral shedders (Knapek *et al.*, 2020). The 12.3-12.5 kb positive-sense RNA genome encodes a polyprotein cleaved into structural (C, E<sup>ms</sup>, E1, E2) and non-structural components (N<sup>pro</sup>, p7, NS2-3, NS4A/B,

NS5A/B) (Wernike and Beer, 2022). BVDV exhibits significant genetic diversity, with two major genotypes (BVDV-1 and BVDV-2) and numerous subgenotypes.

The E2 glycoprotein, a key surface-exposed envelope component of BVDV, critically mediates viral attachment and host cell entry (Leal *et al.*, 2024). As a conserved immunogen, E2 induces neutralizing antibodies and has been widely utilized in DNA vaccines (BVDV-1/-2) and subunit vaccines (full/truncated forms), eliciting robust humoral and cellular immunity against BVDV infection (Couvreux *et al.*, 2007; Chowdhury *et al.*, 2021). Interestingly, the protective effectiveness of the inactivated BVDV-2 vaccine is improved by the addition of recombinant E2 protein (Chung *et al.*, 2018). The E0 or E<sup>ms</sup> protein exhibits high immunogenicity, positioning it as a prime candidate for vaccine engineering. The fusion protein E<sup>ms</sup>-LTB induces a defensive immune response that safeguards against a wide variety of BVDV strains (Wang *et al.*, 2021). The bovine enterovirus (BEV) vector vaccine, which contains the BVDV E0 protein, shows potential as a vaccine for preventing and controlling both

BEV and BVDV by inducing a strong immune response (Ren *et al.*, 2020). More importantly, the recombinant E<sup>rms</sup>-E2 protein induced stronger immune response than either the individual E<sup>rms</sup> or E2 protein in response to BVDV infection (Wang *et al.*, 2020). Virus-like particles (VLP) vaccines incorporating the E<sup>rms</sup>/E2 proteins of BVDV elicit stronger immune responses, both humoral and cellular when compared to inactivated vaccines (Yang *et al.*, 2022).

Effective BVDV control relies on vaccination, biosecurity, and culling of persistently infected (PI) animals. Current vaccines include modified live virus (MLV) and inactivated types, with the latter offering enhanced safety but requiring booster doses for efficacy (Newcomer *et al.*, 2017). MLV vaccines contain attenuated strains of BVDV that stimulate a stronger immune response, although they carry risks of virulence reversion. Given the significant impact of BVDV on global cattle industry, developing safer next-generation vaccines with improved immunogenicity and stability remains imperative.

Multi-epitope vaccines offer distinct advantages over conventional approaches. First, multi-epitope vaccines are designed to target specific T lymphocyte (CTL), helper T lymphocyte (HTL), and B-cell epitopes of a pathogen, excluding non-protective components present in whole-pathogen formulations. Second, by using only selected epitopes, multi-epitope vaccines minimize the risk of adverse reactions associated with certain components of traditional vaccines, such as allergenic or reactogenic components. Furthermore, multi-epitope vaccines possess the ability to simultaneously induce robust cellular and humoral immune responses against specific pathogens (Hammed-Akanmu *et al.*, 2022). Lately, there has been an increasing fascination with studying multi-epitope vaccines for various viruses, including SARS-Cov2 (Ahammad and Lira, 2020), Influenza virus (Rcheulishvili *et al.*, 2023), Monkeypox virus (Suleman *et al.*, 2022), Goatpox virus (Long *et al.*, 2023), and Orf virus (Pang *et al.*, 2024). However, no BVDV-specific multi-epitope vaccine has been reported. This study pioneers an immunoinformatics-driven design of a BVDV subunit vaccine targeting E0/E2 immunogens, systematically evaluating its structural stability and protective potential.

## MATERIALS AND METHODS

**Retrieval of protein sequences:** E0/E2 glycoproteins (GenBank: NP\_776261.1/NP\_776263.1) of the cytopathic reference strain BVDV-1 NADL, and  $\beta$ -defensin-3 adjuvant (GenBank: AAV41025.1) were retrieved from the NCBI database.

**Screening of CTL epitopes:** CD8<sup>+</sup> cytotoxic T lymphocytes (CTLs) mediate antiviral cellular immunity by eliminating infected cells through recognition of MHC-I bound epitopes derived from degraded viral proteins (Reina-Campos *et al.*, 2021). To enable rational vaccine design, 9-mer CTL epitopes from glycoproteins were computationally screened using the IEDB MHC-I tool (Zhang *et al.*, 2023). The NetMHCpan 4.1 EL algorithm was adopted with the following common alleles BoLA-1:00901/00902, BoLA-2:00801, BoLA-4:02401, BoLA-

D18.4, BoLA-HD6, BoLA-T2a, and BoLA-T5 (Wei *et al.*, 2025). CTL epitopes meeting binding score (>0.6) and percentile rank (<0.5%) were filtered. VaxiJen v2.0 (threshold: 0.4) was subsequently utilized to determine the antigenic properties of specific epitopes (Doytchinova and Flower, 2007). ToxinPred was employed for predicting the toxicity of selected epitopes (Gupta *et al.*, 2015).

**Screening of HTL epitopes:** Helper T cells, also known as HTLs or CD4<sup>+</sup> T cells, identify epitopes attached to MHC-II molecules that originate from degraded viral protein fragments. This recognition leads to the activation of both cytotoxic T-cell and B-cell pathways, thereby promoting both cellular and humoral immunity (Habib *et al.*, 2024). Predictions for the 15-mer HTL epitopes from E0/E2 proteins were made using the NetMHCIIpan-2.1 tool (Jensen *et al.*, 2018). Seven highly prevalent BoLA-DRB3 alleles (\*0101, \*0301, \*0303, \*0401, \*0701, \*0901, and \*1101) were prioritized in MHC-II epitope presentation analysis (Wei *et al.*, 2025). HTL epitopes meeting criteria (binding score >0.7, percentile rank <10%) were selected. Antigenicity screening via VaxiJen v2.0 (threshold: 0.4) and subsequent ToxinPred analysis confirmed non-toxicity of prioritized epitopes.

**Screening of B-cell epitopes:** B-cell epitope recognition induces plasma cell differentiation, culminating in pathogen-specific immunoglobulin secretion for immune neutralization (Akkaya *et al.*, 2020). The ABCpred server was utilized to identify potential linear B-cell epitopes (16 mer) of the E0 and E2 proteins at the default threshold of 0.51 (Devarakonda *et al.*, 2023). High-scoring B-cell epitopes (>0.87) were subjected to sequential validation: antigenicity prediction using VaxiJen v2.0 (threshold: 0.4) followed by toxicity screening via ToxinPred.

**Multi-epitope vaccine construction:** A computationally designed BVDV subunit vaccine integrates immunodominant epitopes through category-specific linkers: CTL epitopes (AAY linkers); HTL epitopes (GPGPG); B-cell epitopes (KK). To optimize immune activation, the  $\beta$ -defensin-3 adjuvant was N-terminally fused via an EAAAK linker.

**Comprehensive vaccine characterization:** The multi-epitope vaccine underwent systematic computational profiling: physicochemical properties analysis via ProtParam (Wilkins *et al.*, 1999); Solubility prediction using Protein-Sol (threshold: 0.45) and antigenicity validation with ANTIGENpro with a cutoff 0.4 (Hebditch *et al.*, 2017); Toxicity screening via ToxinPred and allergenicity prediction using AllerTOP2.0 (Gupta *et al.*, 2015).

**Modeling, refining and validating of the multi-epitope vaccine:** PDBsum was used to predict the vaccine's secondary structure, with the Phyre2 tool being employed to establish its 3D representation (Laskowski, 2022). Subsequently, the 3D model was refined by the GalaxyRefine server (Heo *et al.*, 2016). The structural quality of both the original and refined models was assessed using ProSA-Web, with a positive Z-score indicating the presence of erroneous or irregular sections

in the 3D protein models (Wiederstein and Sippl, 2007). Comparative analysis of Ramachandran plots generated by PROCHECK revealed distinct residue distributions across four conformational categories (most favored, additionally allowed, generously permitted, and disallowed regions) between the initial and optimized structural models (Laskowski *et al.*, 1993).

**Molecular docking:** Utilizing the HawkDock molecular docking platform, we quantified the binding kinetics between the chimeric E0-E2 vaccine and bovine TLR2 and TLR4 (AlphaFold:AF-Q95LA9-F1/AF-Q9GL65-F1) (Weng *et al.*, 2019). Binding energy calculations were conducted via the MM/GBSA (Molecular Mechanics/Generalized Born Surface Area) methodology. Subsequent analysis of intermolecular contacts identified key interacted residue clusters between the docked chains through the PDBsum tool (Laskowski *et al.*, 2018).

**Molecular dynamics assessment:** This study used iMODS tool to perform molecular dynamics simulations of the TLR-conjugated immunogens (Lopez-Blanco *et al.*, 2014). The stability of the vaccine receptor complexes model was assessed using Normal Mode Analysis (NMA) and the results were described as deformability plot, B-factor value, eigenvalue, variance, covariance matrix, and elastic network model.

**Immune simulation:** Employing the C-ImmSim computational platform, we performed detailed immune response profiling of the E0-E2 chimeric epitope vaccine (Stolfi *et al.*, 2022). The simulation protocol comprising 1050-time steps with each representing 8 hours. Three-dose immunization was administered at strategic intervals: day 1 (step 1), day 28 (step 84), and day 56 (step 168).

**Codon optimization and virtual cloning:** The chimeric vaccine underwent reverse-translation and *Escherichia coli* K12 codon optimization (JCat tool), with codon adaptation index (CAI) and GC content analysis to validate transcriptional-translational compatibility. Higher CAI values and optimal GC content range of 30-70% generally indicate higher levels of exogenous gene expression (Fadaka *et al.*, 2021). To facilitate vector cloning, *Hind* III/*Xho* I restriction sites were engineered into the cDNA termini for directional cloning into pET-28a(+) using SnapGene.

## RESULTS

**Selection of immunogenic epitopes from the E0/E2 proteins:** Immunodominant epitopes were systematically prioritized through computational immunogenicity screening. CTL epitopes of E0/E2 proteins were predicted via IEDB MHC-I server with stringent criteria: binding score above 0.6, percentile rank below 0.5%, antigenicity exceeding 0.4, and non-toxicity, yielding 7 dominant epitopes (4 from E0, 3 from E2; Table 1). Parallel HTL epitopes were identified using NetMHCIIpan-2.1 with thresholds: prediction score >0.7, antigenicity >0.4, percentile rank <10%, and non-toxicity, resulting in 5 epitopes (2 from E0, 3 from E2; Table 1). Linear B-cell

epitopes were selected through ABCpred with criteria: prediction score >0.87, antigenicity >0.4, and non-toxicity, yielding 7 epitopes for vaccine development (3 from E0, 4 from E2; Table 1). Fig. 1 delineates the computational engineering pipeline for the BVDV multi-epitope vaccine.

### Engineering the BVDV E0-E2 multi-epitope vaccine:

The BVDV E0-E2 multi-epitope vaccine was engineered by fusing 7 CTL, 5 HTL, and 7 linear B-cell epitopes from E0/E2 proteins with  $\beta$ -defensin adjuvant. The vaccine was engineered using AAY (for CTL), GPGPG (for HTL), and KK (B-cell) linkers, where the  $\beta$ -defensin was EAAAK-linked at the N-terminus to boost immunogenicity. Fig. 2 displays the peptide compositional signature of the chimeric E0-E2 vaccine targeting BVDV.

### Comprehensive E0-E2 multi-epitope vaccine characterization:

ProtParam analysis of the constructed E0-E2 multi-epitope vaccine reveals optimal biophysical characteristics: a 357-residue construct (39.35 kDa) with an isoelectric point of 9.66. The protein demonstrates exceptional stability (instability index: 26.60 vs. 40 threshold) and pronounced hydrophilicity (GRAVY: -0.607). Enhanced solubility (0.52 vs. 0.45 cutoff) and strong antigenic potential (0.7374 vs. 0.40 baseline) were confirmed through computational validation. Crucially, comprehensive safety profiling via AllerTOP v2.0 and ToxinPred 1.0 established non-allergenic properties and absence of toxic motifs, fulfilling essential prerequisites for vaccine candidacy.

### Modeling, refining and validating of the E0-E2 multi-epitope vaccine:

Secondary structure of the chimeric E0-E2 vaccine comprises 6 helices (labeled H1-H6), one antiparallel  $\beta$ -sheet including 3 strands (labeled A), 68  $\beta$ -turns, 15  $\gamma$ -turns, one  $\beta$  hairpin, and 2 disulphides (Fig. 3). We employed the phyre2 online platform to predict the 3D model of the vaccine (Fig. 4A). The vaccine's 3D model was subsequently refined through the GalaxyRefine web server, and five optimized 3D models were generated. The refined structural model (Fig. 4B) demonstrated significant improvement in validation parameters, with a GDTHA (Global Distance Test Total Hydrophobic Accessibility) score of 0.8459 accompanied by an RMSD (Root Mean Square Deviation) of 0.655 Å. Quality assessment metrics revealed a MolProbity score of 2.842 and Clash score of 33.5. Comparative analysis through the ProSA web server showed enhanced model quality, as evidenced by the Z-score reduction from -1.59 in the initial model (Fig. 4C) to -2.67 in the optimized structure (Fig. 4D). Ramachandran plot analysis quantified substantial conformational improvements: In the original E0-E2 multi-epitope vaccine model (Fig. 4E), residue distribution comprised 54.6% in the most favored regions (A, B, L), 27.8% in allowed areas (a, b, l, p), 8.1% in marginally permitted zones (~a, ~b, ~l, ~p), and 9.5% in disallowed positions. Post-refinement analysis (Fig. 4F) showed remarkable optimization with 71.9% core region occupancy (+17.3%), 19.3% allowed regions (-8.5%), 2.4% marginally permitted regions (-5.7%), and 6.4% disallowed regions (-3.1%).

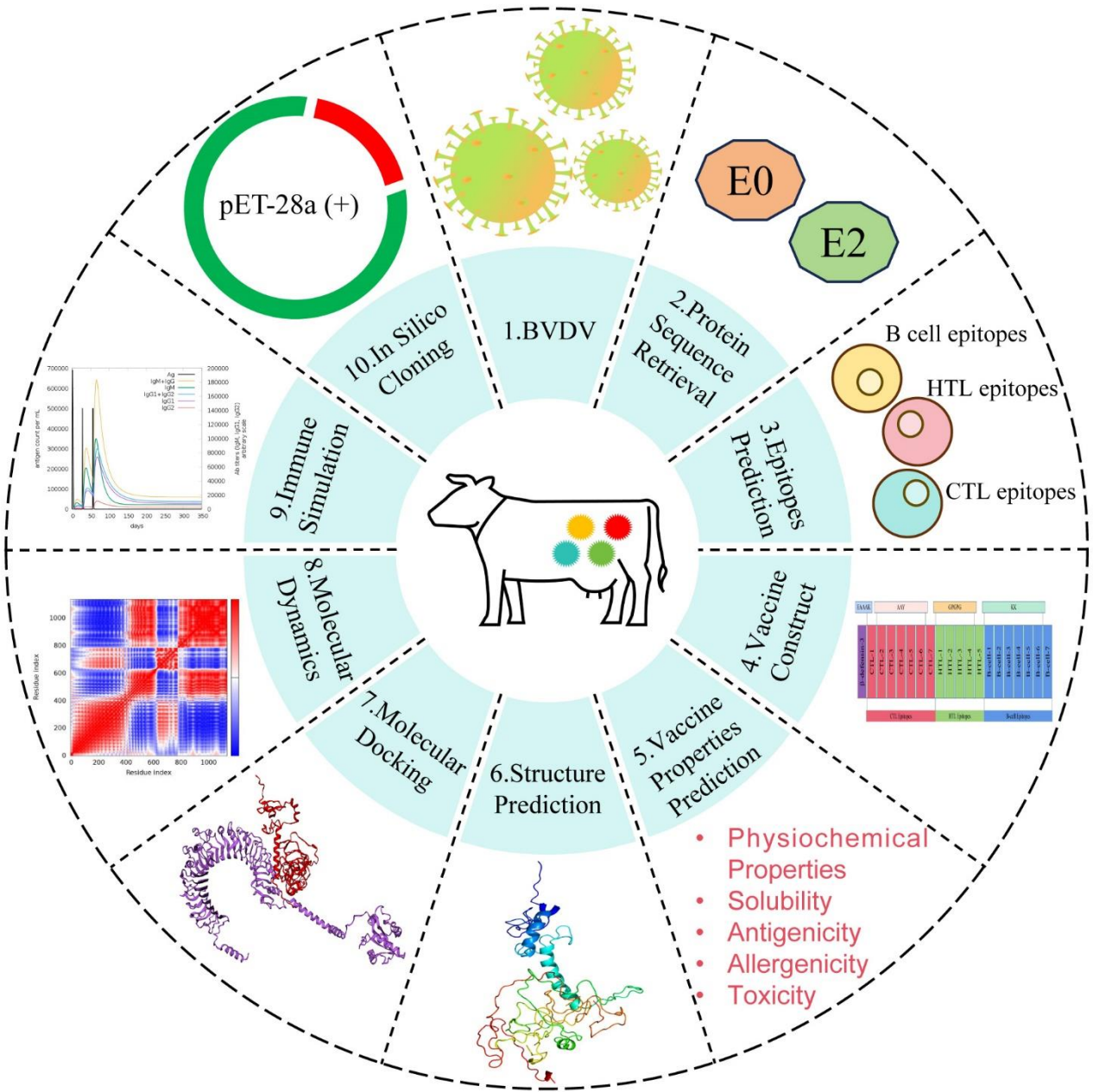
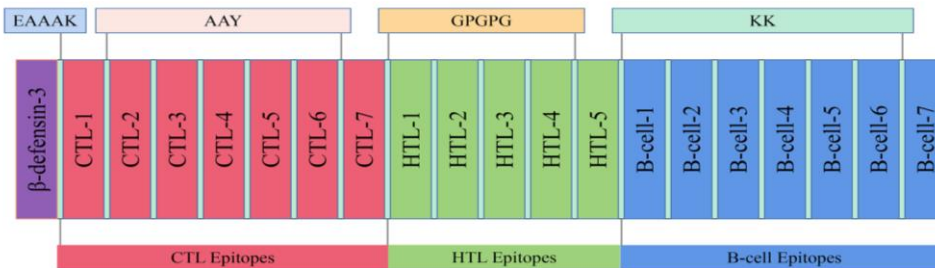


**Fig. 1:** The construction strategy of the chimeric E0-E2 vaccine.

A



B

GIINTLQKYYCRVRGGRCVLSCLPKEEQIGKCSRGRKCCRRKKEAAAK  
 LQRHEWNKHAAYKICTGVP SHAAYCKKGKNFSAAYIAASDVLFKAAAYQQ  
 YMLKGEYAAAYQFKESEGLAAYISSEGPVEK GPGPGPWILVMNRTQANLTE  
 GPGPGQRAMFQRGVNRSLSLHGGPGPGYLAILHTRALPTSVMV GPGPGTVQVIA  
 MDTKLGPMPPGPGPGDGKLMYLRCTRETRKKA VTCRYDRASDLNVTKK  
 ARDSPTPLTGCKKGKNKKLV DGLTNSLEGARQGTKKMLKGEYQYWF DLEV  
 TDKKEDVVMNDNFEFGLCPKKT TTTWKEYSPGMKLEDTKKAIVPQGLKCK  
 KIGKTT

**Fig. 2:** Construction of the chimeric E0-E2 vaccine. (A) Schematic representation of the chimeric E0-E2 vaccine assembly. (B) Peptide compositional signature of the chimeric E0-E2 vaccine. (Purple for β-defensin adjuvant; Red for CTL epitopes; Green for HTL epitopes; Blue for linear B-cell epitopes. Black residues represent the connectors between different elements: EAAAK for β-defensin and CTL epitopes; AAY for CTL epitopes; GPGPG for HTL epitopes; KK for linear B-cell epitopes.)

**Table 1:** CTL, HTL and B-cell epitopes screened for BVDV E0-E2 multi-epitope vaccine construction. Selection criteria comprised: CTL (9-mer; binding score >0.6, percentile rank <0.5%), HTL (15-mer; binding score >0.7, percentile rank <10%), and B-cell epitopes (16-mer; ABCpred >0.85), all maintaining antigenicity score >0.4 and non-toxicity.

Protein	Types	Epitope	Binding alleles	Predicted score	Percentile rank	Antigenicity	Toxicity	
E0	CTL epitopes	71-LQRHEWNKH-79	BoLA-I:00901	0.78	0.09	0.4507	-	
		36-KICTGVPSH-44	BoLA-I:00901	0.68	0.13	0.7987	-	
		138-CKKGNFSF-146	BoLA-D18.4	0.68	0.12	1.4590	-	
		159-IAASDVLFK-167	BoLA-T2a	0.82	0.06	0.5929	-	
	HTL epitopes	88-PWILVMNRTQANLTE-102	BoLA-DRB3*0101	0.777	3.00	0.6973	-	
			BoLA-DRB3*0301	0.665	5.00			
			BoLA-DRB3*0303	0.865	2.00			
			BoLA-DRB3*0901	0.623	4.00			
			BoLA-DRB3*I101	0.806	4.00			
			16-QRAMFQRGVNRSLHG-30	BoLA-DRB3*0101	0.741	5.00	0.5152	-
			BoLA-DRB3*0301	0.758	1.00			
	B-cell epitopes	111-AVTCRYDRASDLNVVT-126 128-ARDSPTPLTGCKKGN-143 182-LVDGLTNSLEGARQGT-197	BoLA-DRB3*0303	0.804	5.00			
			BoLA-DRB3*0901	0.726	0.80			
			BoLA-DRB3*I101	0.735	9.00			
	E2	CTL epitopes	316-QQYMLKGEY-324	BoLA-I:00901	0.81	0.07	0.4845	-
BoLA-I:00902				0.74	0.02			
BoLA-D18.4				0.83	0.04			
BoLA-T5				0.74	0.02			
BoLA-T2a				0.78	0.10			
HTL epitopes		210-YQFKESEGL-218 284-ISSEGPVEK-292 64-YLAHLTRALPTS VV-78	BoLA-D18.4	0.71	0.10	0.8535	-	
			BoLA-HD6	0.81	0.11			
			BoLA-T2a	0.78	0.10	0.9896	-	
			BoLA-DRB3*0101	0.848	0.70	0.4217	-	
			BoLA-DRB3*0301	0.735	1.50			
			BoLA-DRB3*0303	0.735	1.50			
			BoLA-DRB3*0701	0.702	0.40			
B-cell epitopes		262-TVQVIAMD--TKLGMP-276 49-DGKLMYLQRCTRETR-63 319-MLKGEYQYWFLEVTD-334 90-EDVEMNDNFEFGLCP-105 27-TTTWKEYSPGMKLEDT-42 248-AIVPQGTCLKCKIGKTT-263	BoLA-DRB3*0901	0.723	0.90			
			BoLA-DRB3*I101	0.873	0.70			
			BoLA-DRB3*0101	0.711	6.00	0.5545	-	
	BoLA-DRB3*0101		0.700	7.00	0.5227	-		
	BoLA-DRB3*I101		0.762	7.00				
		319-MLKGEYQYWFLEVTD-334		0.93		0.8222	-	
		90-EDVEMNDNFEFGLCP-105		0.88		0.7294	-	
		27-TTTWKEYSPGMKLEDT-42		0.88		0.8372	-	
		248-AIVPQGTCLKCKIGKTT-263		0.87		0.8054	-	

**Molecular docking of vaccine-TLRs:** Computational docking of the E0-E2 chimeric vaccine with bovine TLR2/4 using HawkDock yielded top-ranked models based on docking score and binding affinities. The highest-ranked model for the TLR2-E0-E2 complex demonstrated superior binding (docking score: -6471.12; binding free energy: -44.01 kcal/mol) (Fig. 5A). The optimal model for the TLR4-E0-E2 complex, demonstrated improved binding characteristics (docking score: -7810.60; binding free energy: -57.33 kcal/mol) (Fig. 5B). Visualization and interaction mapping via PDBsum revealed: 2 salt bridges, 4 hydrogen bonds, and 180 non-bonded contacts in TLR2-vaccine interactions (Fig. 5C, 5E). The characterization of interactions in the TLR4-vaccine complex revealed the presence of 4 salt bridges, 6 hydrogen bonds, and 309 non-bonded contacts (Figs. 5D, 5F). The results unequivocally indicated a strong interaction between the E0-E2 chimeric vaccine and bovine TLR2/4.

**Molecular dynamics analysis:** Deformability plot shows the deformability of different atoms in the TLR2/TLR4-BVDV-E0-E2 complexes. Most atoms have low deformability, indicating a stable structure. However, some regions show high deformability peaks, suggesting greater flexibility and susceptibility to deformation during the simulation (Figs. 6A, 6G). B-factor plot displays the thermal motion amplitude of atoms. The red and gray parts represent B-factor values from NMA and experimental PDB, respectively. Overall, B-factor values are low in most regions, indicating stable atomic thermal motion (Figs. 6B,

6H). The eigenvalues plot demonstrates the relative modal stiffness of the vaccine-TLR complexes, and elevated

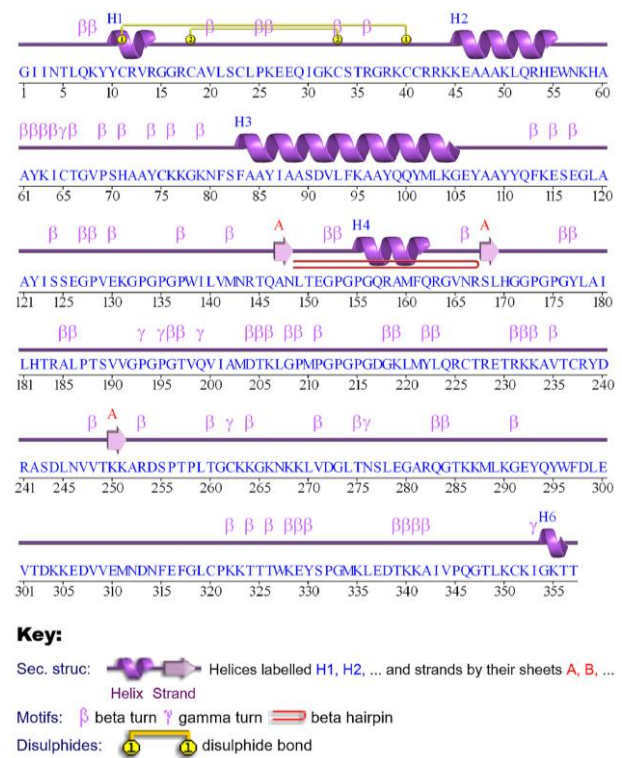


**Fig. 3:** Secondary structure of the chimeric E0-E2 vaccine.

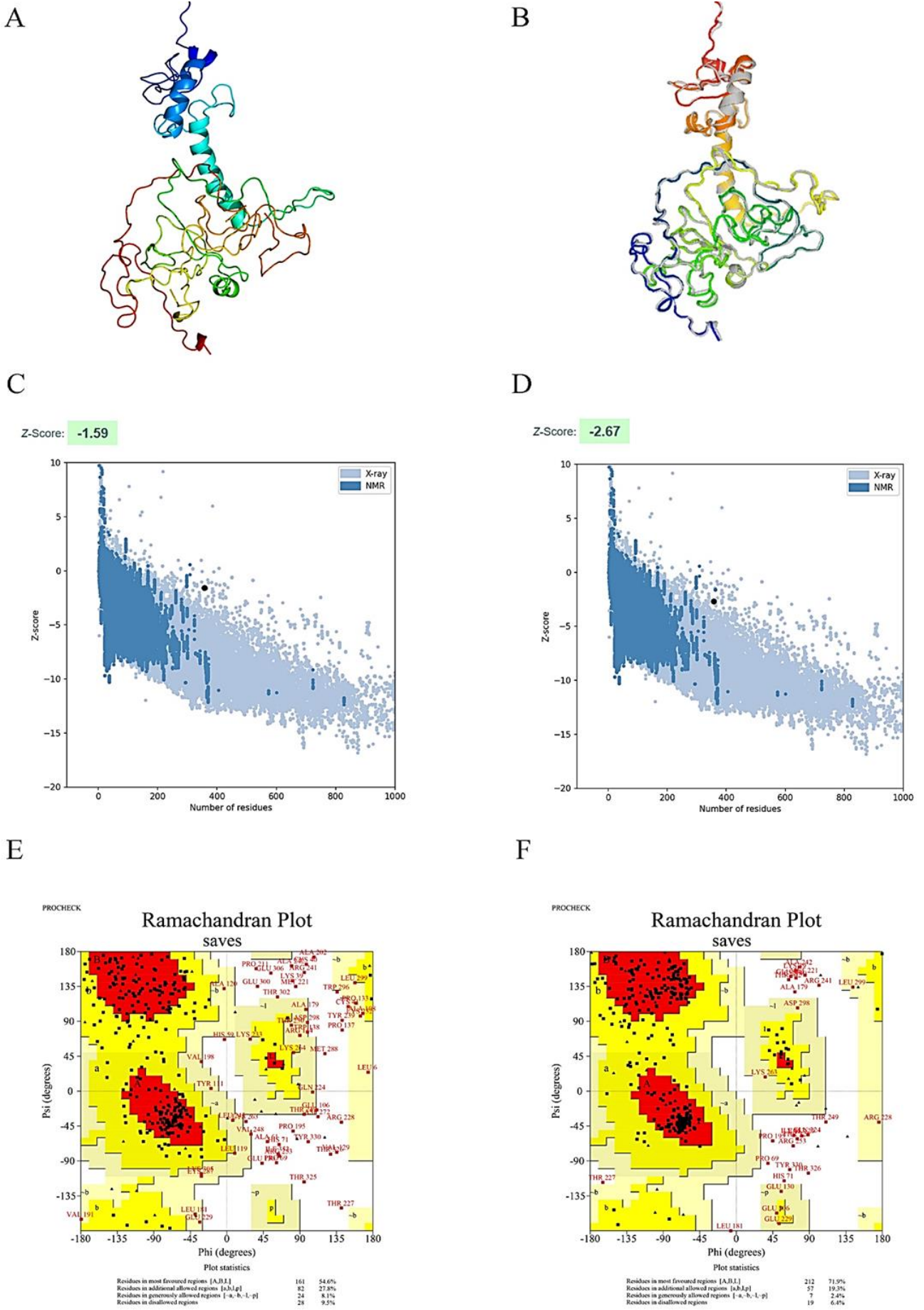


**Fig. 4:** Structural refinement pipeline of the chimeric E0-E2 vaccine. (A) Original 3D structure. (B) Optimized 3D structure. (C, D) Z-scores of both the original and optimized models. (E, F) Ramachandran plots show the distribution of residues located in the most favored, additional allowed, generously allowed, and disallowed regions in both the original and optimized models.

eigenvalues indicate rigid conformational states resistant to perturbation (Figs. 6C, 6I). The variance plot shows the contribution of each mode to the overall variance in the system, with purple and green corresponding to individual and cumulative variances, respectively (Figs. 6D, 6J). The covariance matrix represents the correlated (red), uncorrelated (white), and anti-correlated (blue) motions between residue pairs (Figs. 6E, 6K). The elastic network model provides information on the interactions between atoms in the vaccine-TLR complexes, while the darker gray areas indicate stiffer parts (Figs. 6F, 6L).

**Immune simulation:** Immune simulation of the E0-E2 multi-epitope vaccine demonstrated robust immunogenicity, with IgM titers rising to ~60,000 (IgM+IgG: ~90,000) post-second dose, and peaking at ~100,000 (IgM+IgG: ~180,000) after the third immunization (Fig. 7A). Concomitant increases in IgM/IgM+IgG plasma cells (PLB) mirrored this trend (Fig. 7B). Antigen-driven B cell proliferation was evident through elevated total B cell counts and activated B cell populations following each vaccination (Figs. 7C, 7D). Throughout the simulation period, vaccination significantly increased the number of total helper T cells (TH) and active TH cells, particularly following administration of the E0-E2 multi-epitope subunit vaccine for the second and third time (Figs. 7E, 7F). Additionally, there was a notable increase in the quantity of active cytotoxic T (TC) cells following administration of the E0-E2 multi-epitope subunit vaccine (Fig. 7G). The E0-E2 multi-epitope vaccine elicited marked IFN- $\gamma$  induction (~400,000 ng/mL) post-first/second doses, while the third administration induced relatively less IFN- $\gamma$  production. Concurrently, IL-2 levels peaked at 500,000 ng/mL across all administrations, showing intensified responses after booster doses (Fig. 7H). These data demonstrated that the E0-E2 multi-epitope vaccine effectively induced a robust immune response including both the humoral immunity and cellular immunity.

**Rational codon optimization and cloning:** The vaccine sequence underwent *Escherichia coli* K12 codon optimization, achieving maximal translational efficiency (CAI=1.0) with balanced GC content (50.98%) within the recommended 30-70% range for prokaryotic expression systems (Table 2). These optimized parameters ensure high-level heterologous expression in *E. coli* systems. The codon-optimized E0-E2 gene was subsequently precisely inserted into the pET-28a(+) vector via *Hind* III/*Xho* I restriction cloning, generating the final SnapGene-designed construct (Fig. 8).

## DISCUSSION

This study designed a BVDV subunit vaccine integrating immunodominant E0/E2 epitopes through rational multi-epitope engineering. Computational screening identified 7 CTL, 5 HTL, and 7 B-cell epitopes, strategically fused using AAY/GPGPG/KK linkers to optimize structural stability and epitope presentation

(Humayun *et al.*, 2022). A  $\beta$ -defensin adjuvant, connected via EAAAK linker at the N-terminus, was incorporated to enhance immunogenicity and durability of immune responses (Zhu *et al.*, 2023). The final 357-aa construct displays a significant level of antigenicity and solubility, without any allergenic or toxic properties.

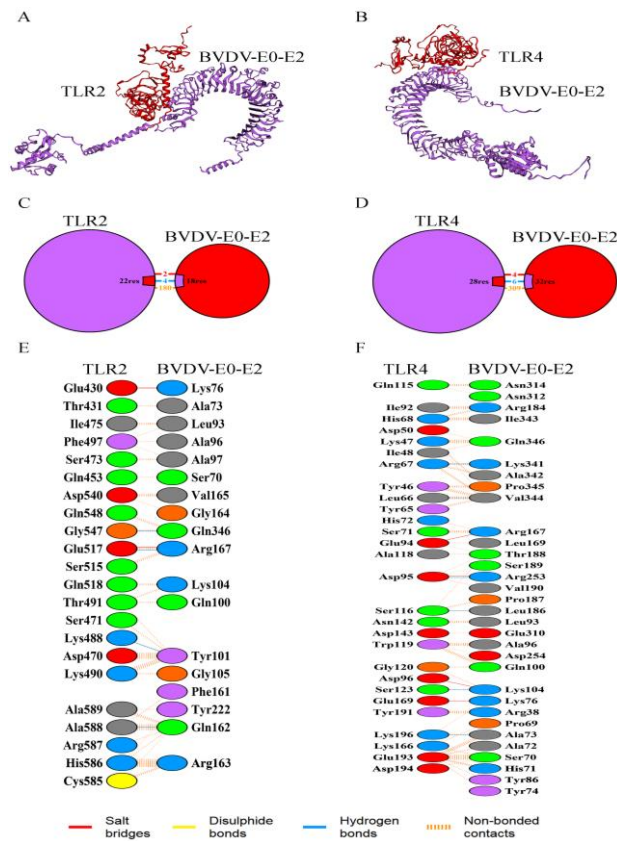


**Fig. 5:** Computational docking of the chimeric E0-E2 vaccine and bovine TLR2/TLR4. (A, B) Interaction patterns between the chimeric E0-E2 vaccine (red) and bovine TLR2/TLR4 (purple). (C, E) Identification of the interacting residues between the chimeric E0-E2 vaccine and TLR2. (D, F) Identification of the interacting residues between the chimeric E0-E2 vaccine and TLR4.

Viral proteins serve as key pathogen-associated molecular patterns (PAMPs), particularly recognized by TLR1/2/4/6/10, which mediate innate antiviral responses (Fitzgerald and Kagan, 2020). TLR2 recognizes human cytomegalovirus glycoprotein B and H, activating NF- $\kappa$ B signaling pathway and inducing proinflammatory cytokines production (Boehme *et al.*, 2006). TLR2/TLR6 heterodimer plays a critical role in modulating the innate immune response to respiratory syncytial virus (RSV) by inducing the production of TNF- $\alpha$ , IL-6, CCL2, and RANTES, which are essential for inhibiting viral replication (Murawski *et al.*, 2009). In addition, TLR2 specifically recognizes the SARS-CoV-2 E protein, inducing proinflammatory cytokine secretion (Zheng *et al.*, 2021). TLR4 demonstrates broad specificity through recognition of some viral glycoproteins, such as RSV F protein and Ebola virus GP (Kurt-Jones *et al.*, 2000; Okumura *et al.*, 2010). We strategically selected these receptors for computational docking analysis with our E0-E2 multi-epitope vaccine construct. Computational docking of our E0-E2 vaccine with bovine TLR2/4 revealed robust receptor-ligand interactions. Immune

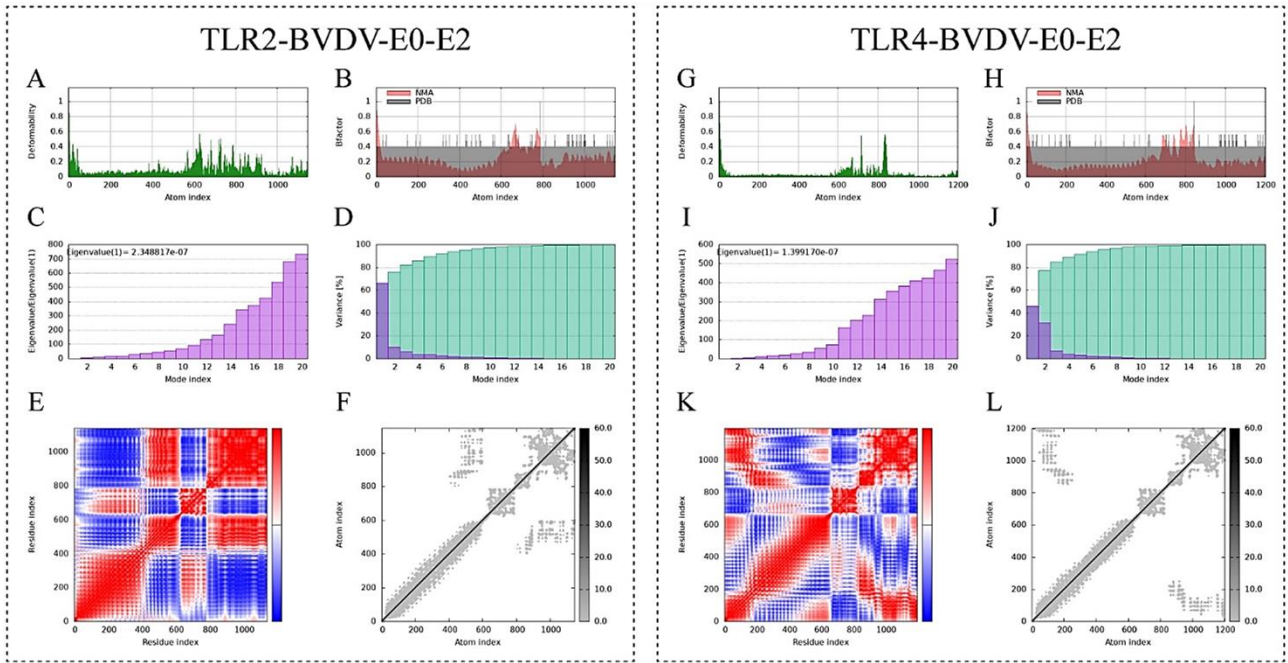


**Fig. 6:** Molecular dynamics profiling of the TLR-BVDV-E0-E2 complexes. (A, G) Structural deformation profiles. (B, H) B-factor distribution heatmap. (C, I) Eigenvalues spectrum analysis. (D, J) Variance analysis plot. (E, K) Covariance matrix plot. (F, L) Elastic network model.

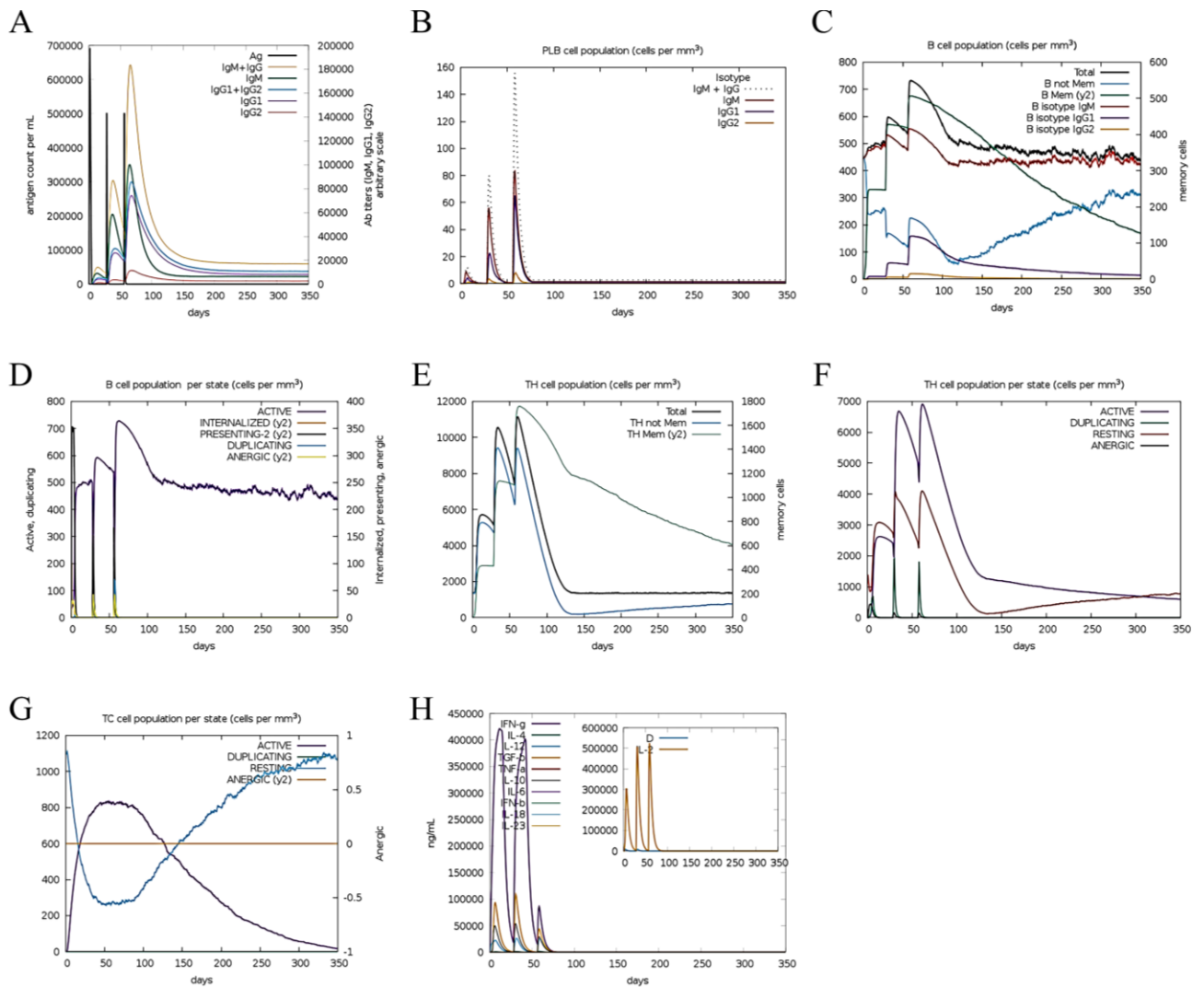


**Fig. 7:** Computational immunogenicity assessment of the chimeric E0-E2 vaccine. (A) Kinetic profiles of IgM and IgG antibody titers. (B) The plasma cells (PLB) isotypes. (C) B cell repertoire quantification. (D) B cell maturation state classification. (E) TH cell quantification. (F) TH cell differentiation status. (G) TC functional state distribution. (H) Cytokine cascade dynamics.

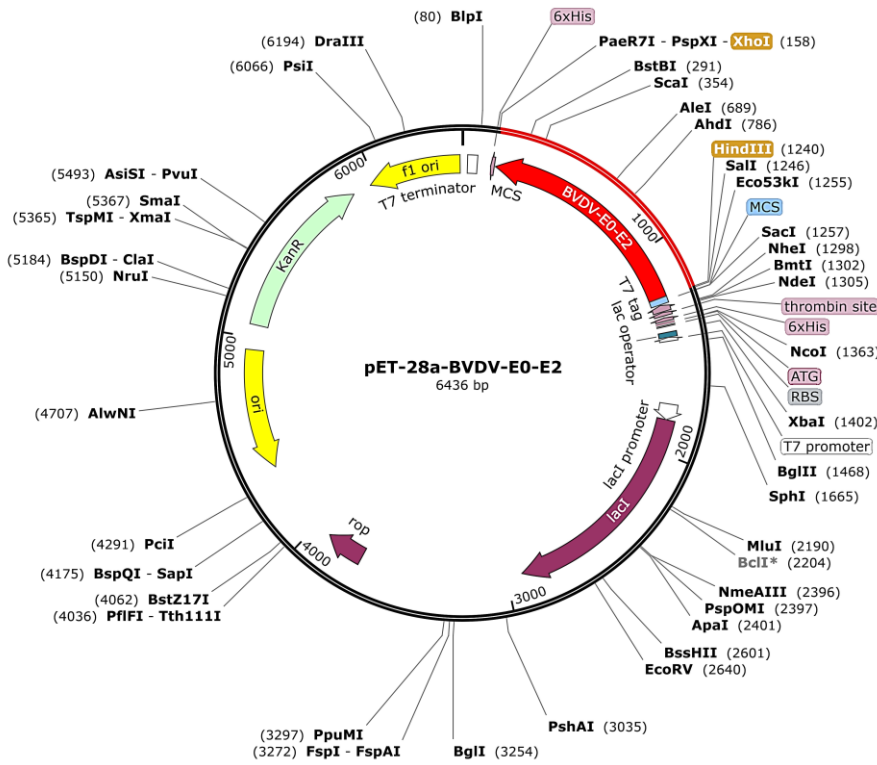


**Fig. 8:** Computational insertion of the chimeric E0-E2 epitope cassette into the pET-28a (+) vector.

**Table 2:** Codon optimization of the BVDV E0-E2 multi-epitope vaccine

Vaccine construct	Protein sequence	Codon optimization ( <i>E.coli</i> K12)
BVDV E0-E2	GIINTLQKYYCRVRGGRCAVL CLPKEEQIGKCSRGRKCCRRK KEAAAKLQRHEWVKHAAAYKI CTGVPSHAAYCKKGNFSAFA YIAASDVLKAAAYQYMLKGEY AAYYQFKESGLAAYSISSEGPVE KGPVGPWILVMNRTQANLTE GPGPGQRAMFQRGVNRSLHG GPGPGYLAILHTRALPTSVVGP PGTVQVIAMDTKLGPMGP GDGKLMYLQRCTRETRKKAVT CRYDRASDLNVVTKKARDSPTP LTGCKKGNKKLVDGLTNSLE GARQGTKKMLKGEYQYWFDL EVTDKKEDVEMNDNFEGFLC PKKTTTWKEYSPGMKLEDTKK AIVPQGLTKCKIGKTT	GGTATCATCAACACCCTGCAGAAATACTACTGCCGTGTTCTGGTGGTTCGCGTGTTC TGTCTTGCCTGCCGAAAGAAGAACAGATCGGTAATGCTCTACCCGTGGTCTGAAATGCTG CCGTTCGTAAGAAAGAGCTGCTGCTAAAACAGCTGACAGCTCACGAATGGAACAAACACGCTGCT TACAAAATCTGCACCGGTGTTCCGTCTCACGCTGCTTACTGCAAAAAGGTAAGAACTTCT CTTTCGCTGCTTACATCGCTGCTTCTGACGTTCTGTTCAAAGCTGCTTACCAGCAGTACATG CTGAAAGGTGAATACGCTGCTTACTACAGTTCAAAGAATCTCGAAGGCTGGGCTGCTTACA TCTCTTCTGAAGGTCCGGTTGAAAAGGTCGGGTCCGGTCCGGTCCGGTATGCTGTTATGAA CCGTACCCAGGCTAACCTGACCGAAGGTCCGGGTCCGGGTCCGGGTACGCTGCTATGTTCCAGCG TGGTGTTAACCGTCTCTGACCGGTGGTCCGGGTCCGGGTACCTGGCTATCCTGCACACC CGTGCTCTGCCGACCTGTTGTTGGTCCGGGTCCGGGTACCGTTACGTTATCGCTATGG ACACCAAACCTGGGTCGGATCCGGGTCCGGGTCCGGGTCCGGGTACCGTAACTGATGATCCTGC AGCGTTGCACCCGTGAAACCCGTAAGAAAGCTGTTACCTGCCGTACCGACCTGCTTCTGA CCTGAACGTTGTTACCAAAAAGCTCGTGACTCTCCGACCCCGCTGACCGGTTGCAAAAAA GGTAAAAACAAAAACTGTTGACGGTCTGACCAACTCTCTGGAAGGTGCTCGTACGGGTA CCAAAAAATGCTGAAAGGTGAATACCAGTACTGGTTCGACCTGGAAGTTACCGACAAAAA AGAAGACGTTGTTGAAATGAACGAACTTGAATCCGGTCTGTGCCCCGAAAAAACACC ACCTGAAAGAATACTCTCCGGGTATGAAACTGGAAGACACCAAAAAGCTATCGTTCCCG AGGGTACCCTGAAATGCAAAATCGGTAAAACCACC

simulations predicted elevated IgG/IgM titers and IFN- $\gamma$ /IL-2 levels, indicative of dual cellular-humoral immunity, positioning it as a hopeful vaccine candidate against BVDV. Among various expression systems like mammalian cells, yeast, and insect cells, *E. coli* stands out as the top prokaryotic choice for its scalability, cost-effectiveness, and simplified purification (Tripathi and Shrivastava, 2019). So, we picked the *E. coli* expression system to produce our multi-epitope vaccine. The vaccine sequence was expertly optimized and ligated into pET-28a (+) vector for high-yield prokaryotic expression. The recombinant protein can be easily purified via nickel affinity chromatography.

While our multi-epitope vaccine candidate has demonstrated strong immunogenic potential in immunoinformatic analyses, the actual protective efficacy against BVDV infection has not been empirically established in biological systems. To bridge this knowledge gap, our subsequent research phase will perform well-controlled challenge-protection trials in

cattle cohorts to evaluate its safety and protective capabilities relative to commercially available inactivated vaccines and modified live virus (MLV) vaccines.

**Conclusions:** A  $\beta$ -defensin-adjuvanted E0-E2 multi-epitope vaccine incorporating 7 CTL, 5 HTL, and 7 B-cell epitopes was designed through immunoinformatics. The vaccine demonstrates favorable solubility and antigenicity, devoid of any allergenic or cytotoxic properties. Furthermore, this candidate vaccine exhibits a high-affinity interaction with the bovine TLR2 and TLR4, leading to a durable and robust immune response in the organism. However, systematic evaluation of the vaccine's safety and protective efficacy is required through phased experimental validation.

**Acknowledgements:** This work was supported by Natural Science Foundation of Guizhou Province, Grant number: ([2022]093).

**Authors contribution:** SL: Software, Methodology, Visualization, Writing-review & editing. MW: Software, Writing-review & editing; WZ: Writing-review & editing; FP: Conceptualization, Writing-original draft, Writing-review & editing, Funding acquisition. All authors have approved the final manuscript.

**Conflict of interest:** None.

## REFERENCES

- Ahammad I and Lira SS, 2020. Designing a novel mRNA vaccine against SARS-CoV-2: An immunoinformatics approach. *Int J Biol Macromol* 162:820-837.
- Akkaya M, Kwak K and Pierce SK, 2020. B cell memory: building two walls of protection against pathogens. *Nat Rev Immunol* 20:229-238.
- Boehme KV, Guerrero M and Compton T, 2006. Human cytomegalovirus envelope glycoproteins B and H are necessary for TLR2 activation in permissive cells. *J Immunol* 177:7094-7102.
- Chowdhury SI, Pannhorst K, Sangewar N, et al., 2021. BoHV-1-Vectored BVDV-2 Subunit Vaccine Induces BVDV Cross-Reactive Cellular Immune Responses and Protects against BVDV-2 Challenge. *Vaccines (Basel)* 9:46.
- Chung YC, Cheng LT, Zhang JY, et al., 2018. Recombinant E2 protein enhances protective efficacy of inactivated bovine viral diarrhoea virus 2 vaccine in a goat model. *BMC Vet Res* 14:194.
- Couvreur B, Letellier C, Olivier F, et al., 2007. Sequence-optimised E2 constructs from BVDV-1b and BVDV-2 for DNA immunisation in cattle. *Vet Res* 38:819-834.
- Devarakonda Y, Reddy M, Neethu RS, et al., 2023. Multi epitope vaccine candidate design against *Streptococcus pneumoniae*. *J Biomol Struct Dyn* 41:12654-12667.
- Doytchinova IA and Flower DR, 2007. Vaxijen: a server for prediction of protective antigens, tumour antigens and subunit vaccines. *BMC Bioinformatics* 8:4.
- Fadaka AO, Sibuyi NRS, Martin DR, et al., 2021. Immunoinformatics design of a novel epitope-based vaccine candidate against dengue virus. *Sci Rep* 11:19707.
- Fitzgerald KA and Kagan JC, 2020. Toll-like Receptors and the Control of Immunity. *Cell* 180:1044-1066.
- Gupta S, Kapoor P, Chaudhary K, et al., 2015. Peptide toxicity prediction. *Methods Mol Biol* 1268:143-157.
- Habib A, Liang Y, Xu X, et al., 2024. Immunoinformatic Identification of Multiple Epitopes of gp120 Protein of HIV-1 to Enhance the Immune Response against HIV-1 Infection. *Int J Mol Sci* 25:2432.
- Hammed-Akanmu M, Mim M, Osman AY, et al., 2022. Designing a Multi-Epitope Vaccine against *Toxoplasma gondii*: An Immunoinformatics Approach. *Vaccines (Basel)* 10:1389.
- Hebditch M, Carballo-Amador MA, Charonis S, et al., 2017. Protein-Sol: a web tool for predicting protein solubility from sequence. *Bioinformatics* 33:3098-3100.
- Heo L, Lee H and Seok C, 2016. GalaxyRefineComplex: Refinement of protein-protein complex model structures driven by interface repacking. *Sci Rep* 6:32153.
- Humayun F, Cai Y, Khan A, et al., 2022. Structure-guided design of multi-epitopes vaccine against variants of concern (VOCs) of SARS-CoV-2 and validation through In silico cloning and immune simulations. *Comput Biol Med* 140:105122.
- Jensen KK, Andreatta M, Marcatili P, et al., 2018. Improved methods for predicting peptide binding affinity to MHC class II molecules. *Immunology* 154:394-406.
- Knappek KJ, Georges HM, Van Campen H, et al., 2020. Fetal Lymphoid Organ Immune Responses to Transient and Persistent Infection with Bovine Viral Diarrhoea Virus. *Viruses* 12:816.
- Kurt-Jones EA, Popova L, Kwinn L, et al., 2000. Pattern recognition receptors TLR4 and CD14 mediate response to respiratory syncytial virus. *Nat Immunol* 1:398-401.
- Lanyon SR, Hill FI, Reichel MP, et al., 2014. Bovine viral diarrhoea: pathogenesis and diagnosis. *Vet J* 199:201-209.
- Laskowski RA, 2022. PDBsum1: A standalone program for generating PDBsum analyses. *Protein Sci* 31:e4473.
- Laskowski RA, Jablonska J, Pravda L, et al., 2018. PDBsum: Structural summaries of PDB entries. *Protein Sci* 27:129-134.
- Laskowski RA, MacArthur MV, Moss DS, et al., 1993. PROCHECK: a program to check the stereochemical quality of protein structures. *J Appl Crystallogr* 26:283-291.
- Leal ES, Pascual MJ, Adler NS, et al., 2024. Unveiling tetrahydroquinolines as promising BVDV entry inhibitors: Targeting the envelope protein. *Virology* 590:109968.
- Long Q, Wei M, Wang Y, et al., 2023. Design of a multi-epitope vaccine against goatpox virus using an immunoinformatics approach. *Front Cell Infect Microbiol* 13:1309096.
- Lopez-Blanco JR, Aliaga JI, Quintana-Orti ES, et al., 2014. iMODS: internal coordinates normal mode analysis server. *Nucleic Acids Res* 42:W271-W276.
- Mirosław P, Rola-Luszczak M, Kuzmak J, et al., 2022. Transcriptomic Analysis of MDBK Cells Infected with Cytopathic and Non-Cytopathic Strains of Bovine Viral Diarrhoea Virus (BVDV). *Viruses* 14:1276.
- Murawski MR, Bowen GN, Cerny AM, et al., 2009. Respiratory syncytial virus activates innate immunity through Toll-like receptor 2. *J Virol* 83:1492-1500.
- Newcomer BW, 2021. 75 years of bovine viral diarrhoea virus: Current status and future applications of the use of directed antivirals. *Antiviral Res* 196:105205.
- Newcomer BW, Chamorro MF and Walz PH, 2017. Vaccination of cattle against bovine viral diarrhoea virus. *Vet Microbiol* 206:78-83.
- Okumura A, Pitha PM, Yoshimura A, et al., 2010. Interaction between Ebola virus glycoprotein and host toll-like receptor 4 leads to induction of proinflammatory cytokines and SOCS1. *J Virol* 84:27-33.
- Pang F, Long Q and Liang S, 2024. Designing a multi-epitope subunit vaccine against Orf virus using molecular docking and molecular dynamics. *Virulence* 15:2398171.
- Rcheulishvili N, Mao J, Papukashvili D, et al., 2023. Designing multi-epitope mRNA construct as a universal influenza vaccine candidate for future epidemic/pandemic preparedness. *Int J Biol Macromol* 226:885-899.
- Reina-Campos M, Scharping NE and Goldrath AW, 2021. CD8(+) T cell metabolism in infection and cancer. *Nat Rev Immunol* 21:718-738.
- Ren X, Zhang S, Gao X, et al., 2020. Experimental immunization of mice with a recombinant bovine enterovirus vaccine expressing BVDV E0 protein elicits a long-lasting serologic response. *Virol J* 17:88.
- Stoffi P, Castiglione F, Mastrostefano E, et al., 2022. In-silico evaluation of adenoviral COVID-19 vaccination protocols: Assessment of immunological memory up to 6 months after the third dose. *Front Immunol* 13:998262.
- Suleman M, Rashid F, Ali S, et al., 2022. Immunoinformatic-based design of immune-boosting multi-epitope subunit vaccines against monkeypox virus and validation through molecular dynamics and immune simulation. *Front Immunol* 13:1042997.
- Tripathi NK and Shrivastava A, 2019. Recent Developments in Bioprocessing of Recombinant Proteins: Expression Hosts and Process Development. *Front Bioeng Biotechnol* 7:420.
- Wang S, Yang G, Nie J, et al., 2020. Recombinant E(rns)-E2 protein vaccine formulated with MF59 and CPG-ODN promotes T cell immunity against bovine viral diarrhoea virus infection. *Vaccine* 38:3881-3891.
- Wang SH, Yang GH, Nie JW, et al., 2021. Immunization with recombinant E(rns)-LTB fusion protein elicits protective immune responses against bovine viral diarrhoea virus. *Vet Microbiol* 259:109084.
- Wei M, Liang S, Wang Y, et al., 2025. Design and assessment of two broad-spectrum multi-epitope vaccine candidates against bovine viral diarrhoea virus based on the E0 or E2 envelope glycoprotein. *Vet J* 309:106296.
- Weng G, Wang E, Wang Z, et al., 2019. HawkDock: a web server to predict and analyze the protein-protein complex based on computational docking and MM/GBSA. *Nucleic Acids Res* 47:W322-W330.
- Wernike K and Beer M, 2022. International proficiency trial for bovine viral diarrhoea virus (BVDV) antibody detection: limitations of milk serology. *BMC Vet Res* 18:168.
- Wiederstein M and Sippl MJ, 2007. ProSA-web: interactive web service for the recognition of errors in three-dimensional structures of proteins. *Nucleic Acids Res* 35:W407-W410.
- Wilkins MR, Gasteiger E, Bairoch A, et al., 1999. Protein identification and analysis tools in the ExPASy server. *Methods Mol Biol* 112:531-552.
- Yang N, Zhang J, Xu M, et al., 2022. Virus-like particles vaccines based on glycoprotein E0 and E2 of bovine viral diarrhoea virus induce Humoral responses. *Front Microbiol* 13:1047001.
- Zhang G, Han L, Zhao Y, et al., 2023. Development and evaluation of a multi-epitope subunit vaccine against *Mycoplasma synoviae* infection. *Int J Biol Macromol* 253:126685.
- Zheng M, Karki R, Williams EP, et al., 2021. TLR2 senses the SARS-CoV-2 envelope protein to produce inflammatory cytokines. *Nat Immunol* 22:829-838.
- Zhu F, Tan C, Li C, et al., 2023. Design of a multi-epitope vaccine against six *Nocardia* species based on reverse vaccinology combined with immunoinformatics. *Front Immunol* 14:1100188.